Available online at www.sciencedirect.com
SCIENCE DIRECT®
Journal of Sound and Vibration 279 (2005) 619–639
JOURNAL OF SOUND AND VIBRATION
www.elsevier.com/locate/jsvi

A non-linear model for the dynamics of an inclined cable

A. Berlioz[a,*,1], C.-H. Lamarque[b]

[a] *Laboratoire de Dynamique des Machines et des Structures UMR5006, Institut National des Sciences Appliquées de Lyon, F69621 Villeurbanne, France*

[b] *Laboratoire GéoMatériaux URA 1652, Ecole Nationale des Travaux Publics de l'Etat, F69518 Vaulx-en-Velin Cedex, France*

Received 11 February 2003; accepted 11 November 2003

Abstract

This article is devoted to the theoretical and experimental investigations of an inclined cable subjected to the boundary motion condition. A model is presented for predicting non-linear behaviour. The analysis of basic phenomena is performed using the multiple scales method. The cable is modelled with one or two degrees of freedom for in-plane displacement. Models with one or two degrees of freedom are used for out-of-plane displacements. Experiments are carried out on the mechanical model and served to identify parameters and validate the one-degree of freedom model for in-plane displacements. Numerical and experimental results are in good agreement.

1. Introduction

Numerous papers have been devoted to the study of cable vibrations. This is not surprising since the study of cable dynamics is important and difficult at the theoretical level (hyperbolic models [1]) and for practical applications (cable-stayed bridges, rope-ways [2], inextensible whirling strings [3], etc.). Qualitative and quantitative information about the physics of cables are useful for applications stemming from discrete models and sophisticated numerical models (Finite Element approaches, etc.) In order to lay out cable structures a theoretical, numerical and

*Corresponding author. UFR-MIG Département de Mécanique, Bat 1R2, Université Paul Sabatier Toulouse III, 118, route de Narbonne, 31062 Toulouse, Cedex 4, France. Tel.: +33-5-61-55-63-75; fax: +33-5-61-55-83-26.

E-mail address: berlioz@lm2f.ups-tlse.fr (A. Berlioz).

[1] Present address: Laboratoire de Génie Mécanique de Toulouse EA814, Université Paul Sabatier, 31062 Toulouse, France.

0022-460X/$ - see front matter
doi:10.1016/j.jsv.2003.11.069

experimental study of cable damper systems and their effects on non-linear vibrations is presented in Refs. [4,5]. See also Ref. [6] for the control of cables with active tendons.

Irvine and Caughey [7] did not take into account the quadratic and cubic terms of the partial differential equations governing the three-dimensional vibrations of a cable. They considered a linear simplified model. In Ref. [8], Irvine studied a linear model (flat-sag cable) that permitted him to solve the vibration problem completely and introduced the non-linear model of a taut-flat cable, though without solving it. The study of a non-linear model was carried out by Carrier, using specific boundary conditions [9,10]. Meirovitch [11] showed that the undamped non-linear steady state in a plane response of a taut flat cable is given by the solution of a Duffing equation. West et al. [12] or Henghold and Russell [13] also studied natural frequencies of cable structures. Hence it is clear that cable vibrations have to be studied in the framework of non-linear mechanics.

Nayfeh and Mook [14] reviewed recalled the basic modelling for strings and provide many references on the topic. Takahashi and Konishi [15,16] presented non-linear free vibrations and forced responses for a three dimensional case. Benedettini and Rega [17–19] and Benedettini et al. [20] studied planar non-linear oscillations of an elastic cable suspended between two fixed supports at the same level under several different resonance conditions. They presented experimental, analytical and numerical results. Benedettini et al. [21] investigated a four-degree-of-freedom model of a suspended cable; again Rega et al. [22] considered multi-modal resonances in a suspended cable studied using a perturbation approach. Non-linear mode interactions were also investigated by Pilipchuk and Ibrahim for a horizontal cable [23]. Zheng et al. [24] considered the super-harmonics and internal resonance of a suspended cable with almost commensurable natural frequencies.

The global bifurcation of strings was investigated by O'Reilly [25]. Vibrations due to the parametric excitation of a cable stayed structure have been investigated by Lilien and Costa [26]. Fujino et al. [27] built a 3 d.o.f. model of a cable-stayed beam and compared the results of analytical approaches with experimental results. In his PhD thesis, Khadaroui [28] proposed several models for simplified cable stayed bridges with at most 3 d.o.f. In particular he introduced a one degree-of-freedom model of an inclined cable subjected to an external excitation corresponding to the movement of the deck of the bridge. In this paper a revised version of the simplified model given by Khadroui [28] is provided. Zhao et al. [29] dealt with a two-degree-of-freedom model of an inclined cable for a theoretical investigation of in-plane and out-of-plane motions approximated by the first in-plane and out-of-plane modes. Nielsen and Kierkegaard [30] also investigated simplified models of inclined cables under super and combinatorial harmonic excitation: they gave analytical and purely numerical results.

Raouf [31] reviewed the literature and results on the response of cables under stochastic excitation and on the comparison between analytical (simplified) results and purely numerical results for approximated models, which are sometimes compared with experimental results.

In comparison with the above literature, an inclined cable subjected to external sinusoidal forcing leading to primary and sub-harmonic resonances is considered here. The work presented here concerns models with a few degrees of freedom obtained by projecting the continuous model onto a finite number of linear modes, the (quantitative) comparison between experimental investigations of planar motions and analytical results obtained for the simplified one degree-of-freedom non-linear model, and the (qualitative) comparison between experimental results for

non-planar motions and analytical results (two degree-of-freedom model). It extends and improves previous work [32].

2. Modellization

Following on from the studies reported by Fujino [27] and Khadraoui [28], a non-linear model of a cable coupled to a horizontal beam as a simplified model of a cable stayed-bridge is considered. This work studies the vibrations of an inclined single cable by using a reduced model (using experimental and numerical analyses). At equilibrium position, the cable is fixed at its ends A and B, so that its chord defines angle θ versus horizontal axis Ox. Planar oscillations are considered in an Oxy frame where the axis Oy is perpendicular to Ox (see Fig. 1). Non-planar oscillations can occur in direction Oz, so that $Oxyz$ forms a direct orthogonal frame. The vibrations of the cable around its equilibrium position are studied and its curvature is taken into account.

Taking as basis the assumption of small displacements and large deformations for an inclined cable, a non-linear model is built by three coupled partial differential equations [8]:

$$\begin{aligned} m_c\frac{\partial^2 U}{\partial t^2} - m_c g\sin\theta &= \frac{\partial}{\partial s}\left((T+\tau)\left(\frac{\mathrm{d}X}{\mathrm{d}s}+\frac{\partial U}{\partial s}\right)\right),\\ m_c\frac{\partial^2 V}{\partial t^2} - m_c\, g\cos\theta &= \frac{\partial}{\partial s}\left((T+\tau)\left(\frac{\mathrm{d}Y}{\mathrm{d}s}+\frac{\partial V}{\partial s}\right)\right),\\ m_c\frac{\partial^2 W}{\partial t^2} &= \frac{\partial}{\partial s}\left((T+\tau)\left(\frac{\partial W}{\partial s}\right)\right), \end{aligned} \tag{1}$$

where m_c is the mass of the cable per unit length, $g = 9.81\,\mathrm{m\,s^{-2}}$. T is the tension at static equilibrium. τ is the variation of tension corresponding to the movement of a point located at $(X, Y, 0)$ (static equilibrium position) expressed in the local frame by $(X+U, Y+V, W)$, U is being the displacement parallel to the initial chord, V is the displacement orthogonal to U in the cable plane while W is the out-of-plane displacement (see Fig. 1), and s is the curvilinear abscissa. The following non-dimensional constants are introduced:

$$\begin{aligned} &s = \bar{s}L, \quad X = \bar{X}L, \quad Y = \bar{Y}L, \quad U = \bar{U}L, \quad V = \bar{V}L,\\ &W = \bar{W}L, \quad T = \bar{T}H, \quad \tau = \bar{\tau}H, \quad \bar{t} = \frac{\sqrt{H/m_c}}{L}t, \end{aligned} \tag{2}$$

where L is the cable span and H is the horizontal component of the tension at static equilibrium. Then, using Hooke's non-dimensional law in the form:

$$\tau = \xi\varepsilon_{def} \tag{3}$$

with a Green–Lagrange deformation

$$\varepsilon_{def} = \frac{\mathrm{d}\bar{X}}{\mathrm{d}\bar{s}}\frac{\partial\bar{U}}{\partial\bar{s}} + \frac{\mathrm{d}\bar{Y}}{\mathrm{d}\bar{s}}\frac{\partial\bar{V}}{\partial\bar{s}} + \frac{1}{2}\left[\left(\frac{\partial\bar{U}}{\partial\bar{s}}\right)^2 + \left(\frac{\partial\bar{V}}{\partial\bar{s}}\right)^2 + \left(\frac{\partial\bar{W}}{\partial\bar{s}}\right)^2\right] \tag{4}$$

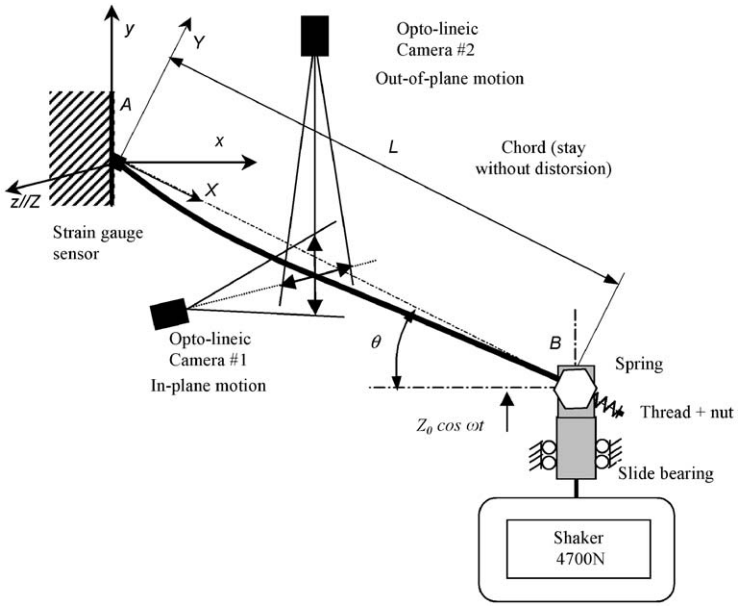

Fig. 1. Schematic diagram of the experimental set-up.

with $\xi = \xi_0 \cos\theta$ and $\xi_0 = ES/H$ where E and S are the Young modulus and the area of the cable respectively. See Appendix A for other definitions.The final model is then obtained:

$$
\begin{aligned}
&\frac{\partial^2 \bar{U}}{\partial \bar{t}^{\,2}} - \frac{\partial}{\partial \bar{s}}\left[\left(\bar{T}(s) + \xi\left(\frac{\mathrm{d}\bar{X}}{\mathrm{d}\bar{s}}\right)^2\right)\frac{\partial \bar{U}}{\partial \bar{s}} + \xi\frac{\mathrm{d}\bar{X}}{\mathrm{d}\bar{s}}\frac{\mathrm{d}\bar{Y}}{\mathrm{d}\bar{s}}\frac{\partial \bar{V}}{\partial \bar{s}}\right] \\
&\quad - \xi\frac{\partial}{\partial \bar{s}}\left[\left(\frac{\mathrm{d}\bar{X}}{\mathrm{d}\bar{s}}\frac{\partial \bar{U}}{\partial \bar{s}} + \frac{\mathrm{d}\bar{Y}}{\mathrm{d}\bar{s}}\frac{\partial \bar{V}}{\partial \bar{s}}\right)\frac{\partial \bar{U}}{\partial \bar{s}} + \frac{1}{2}\left(\left(\frac{\partial \bar{U}}{\partial \bar{s}}\right)^2 + \left(\frac{\partial \bar{V}}{\partial \bar{s}}\right)^2 + \left(\frac{\partial \bar{W}}{\partial \bar{s}}\right)^2\right)\right]\left(\frac{\mathrm{d}\bar{X}}{\mathrm{d}\bar{s}} + \frac{\partial \bar{U}}{\partial \bar{s}}\right) = 0, \\
&\frac{\partial^2 \bar{V}}{\partial \bar{t}^{\,2}} - \frac{\partial}{\partial \bar{s}}\left[\left(\bar{T}(s) + \xi\left(\frac{\mathrm{d}\bar{Y}}{\mathrm{d}\bar{s}}\right)^2\right)\frac{\partial \bar{V}}{\partial \bar{s}} + \xi\frac{\mathrm{d}\bar{X}}{\mathrm{d}\bar{s}}\frac{\mathrm{d}\bar{Y}}{\mathrm{d}\bar{s}}\frac{\partial \bar{U}}{\partial \bar{s}}\right] \\
&\quad - \xi\frac{\partial}{\partial \bar{s}}\left[\left(\frac{\mathrm{d}\bar{X}}{\mathrm{d}\bar{s}}\frac{\partial \bar{U}}{\partial \bar{s}} + \frac{\mathrm{d}\bar{Y}}{\mathrm{d}\bar{s}}\frac{\partial \bar{V}}{\partial \bar{s}}\right)\frac{\partial \bar{V}}{\partial \bar{s}} + \frac{1}{2}\left(\left(\frac{\partial \bar{U}}{\partial \bar{s}}\right)^2 + \left(\frac{\partial \bar{V}}{\partial \bar{s}}\right)^2 + \left(\frac{\partial \bar{W}}{\partial \bar{s}}\right)^2\right)\right]\left(\frac{\mathrm{d}\bar{Y}}{\mathrm{d}\bar{s}} + \frac{\partial \bar{V}}{\partial \bar{s}}\right) = 0, \\
&\frac{\partial^2 \bar{W}}{\partial \bar{t}^{\,2}} - \frac{\partial}{\partial \bar{s}}\left[\bar{T}(s)\frac{\partial \bar{W}}{\partial \bar{s}}\right] \\
&\quad - \xi\frac{\partial}{\partial \bar{s}}\left[\left(\frac{\mathrm{d}\bar{X}}{\mathrm{d}\bar{s}}\frac{\partial \bar{U}}{\partial \bar{s}} + \frac{\mathrm{d}\bar{Y}}{\mathrm{d}\bar{s}}\frac{\partial \bar{V}}{\partial \bar{s}}\right)\frac{\partial \bar{W}}{\partial \bar{s}} + \frac{1}{2}\left(\left(\frac{\partial \bar{U}}{\partial \bar{s}}\right)^2 + \left(\frac{\partial \bar{V}}{\partial \bar{s}}\right)^2 + \left(\frac{\partial \bar{W}}{\partial \bar{s}}\right)^2\right)\right]\frac{\partial \bar{W}}{\partial \bar{s}} = 0,
\end{aligned}
\tag{5}
$$

with the boundary conditions $U(0,t) = 0$, $V(0,t) = 0$, $W(0,t) = 0$ at A and $(U(L,t) = -Z_0 \cos\omega t \sin\theta)$, $V(L,t) = Z_0 \cos\omega t \cos\theta$, $W(L,t) = 0$ at B.

2.1. Simplified model with one degree-of-freedom

The longitudinal displacements are neglected and the vibrations of the first planar mode of the cable are studied. The dimensional displacement V can be written in the form:

$$V(X,t) = f(X)\varphi(t) + \frac{X}{L} Z_0 \cos\theta \cos\omega t \tag{6}$$

so that the boundary conditions at both extremities are satisfied. The Irvine function $f(X)$ providing the vibration according to the first planar mode and verifying the geometrical boundary conditions at the end of the cable [8] is given by

$$f\left(\frac{X}{L}\right) = \frac{\left(1 - \cos\left(\omega_0 \frac{X}{L}\right) - \tan\left(\frac{\omega_0}{2}\right)\sin\left(\omega_0 \frac{X}{L}\right)\right)}{\left(1 - \cos\left(\frac{\omega_0}{2}\right) - \tan\left(\frac{\omega_0}{2}\right)\sin\left(\frac{\omega_0}{2}\right)\right)} \tag{7}$$

and $\varphi(t)$ is an unknown modal coordinate.

Using non-dimensional variables, but omitting overbars to simplify the notation and since

$$\frac{\partial U}{\partial X} \ll 1 \quad \text{and} \quad \frac{\partial U}{\partial X} \ll \frac{\partial V}{\partial X} \tag{8}$$

the following equation governing the motion of the cable by using the Ritz–Galerkin method is obtained (with the overbar omitted for φ and Ω derived from ω via the non-dimensional time):

$$\begin{aligned} &\ddot{\varphi} + 2e\omega_0\dot{\varphi} + \omega_0^2\varphi + b_1\varphi^2 + b_2\varphi^3 + b_3\cos(\Omega t)\varphi + b_4\cos^2(\Omega t)\varphi \\ &\quad = b_5\cos(\Omega t) + b_6\cos^2(\Omega t) + b_7\sin(\Omega t) \end{aligned} \tag{9}$$

with reduced damping e (obtained experimentally via logarithmic decrement) and

$$\omega_0^2 = \frac{C_1}{C_0} + \xi\frac{C_2^2}{C_0}, \tag{10}$$

where C_0, C_1, C_2, C_3 and b_1–b_7 are given in Appendix A.

2.2. Simplified model with 2 d.o.f.

Following the same procedure, as in the previous section, it is possible to develop models of a cable with 2 (or more) degrees of freedom for example, seeking vibrations that include the first in-plane and the first out-of-plane modes. The dimensional displacements V and W can be written in the form:

$$V(X,t) = f_y(X)\varphi_y(t) + \frac{X}{L} Z_0 \cos\theta \cos\omega t, \tag{11}$$

$$W(X,t) = f_z(X)\varphi_z(t) \tag{12}$$

so that the boundary conditions at both extremities are satisfied. The Irvine functions f_y and f_z for the first in-plane mode and the first out-of-plane mode respectively are defined

by [8]:

$$f_y\left(\frac{X}{L}\right) = \frac{\left(1-\cos\left(\omega_0\frac{X}{L}\right)-\tan\left(\frac{\omega_0}{2}\right)\sin\left(\omega_0\frac{X}{L}\right)\right)}{\left(1-\cos\left(\frac{\omega_0}{2}\right)-\tan\left(\frac{\omega_0}{2}\right)\sin\left(\frac{\omega_0}{2}\right)\right)}, \tag{13}$$

$$f_z\left(\frac{X}{L}\right) = \sin\left(\frac{\pi X}{L}\right). \tag{14}$$

As was done for Eq. (9), the following non-dimensional equations governing the motion of the cable are obtained (with the overbar omitted for φ_y and φ_z):

$$\begin{aligned}&\ddot{\varphi}_y + A1\dot{\varphi}_y + A2\varphi_y + A3\cos(\Omega t)\varphi_y + A4\cos^2(\Omega t)\varphi_y + A5\varphi_y^3 + A6\varphi_y^2 + A7\varphi_z^2 + A8\varphi_z^2\varphi_y\\ &\quad = -A9\cos(\Omega t) - A10\cos^2(\Omega t) - A11\Omega\sin(\Omega t) - A12\Omega^2\cos(\Omega t),\end{aligned} \tag{15}$$

$$\ddot{\varphi}_z + B1\dot{\varphi}_z + B2\varphi_z + B3\cos(\Omega t)\varphi_z + B4\cos^2(\Omega t)\varphi_z + B5\varphi_z^3 + B6\varphi_y\varphi_z + B7\varphi_y^2\varphi_z = 0, \tag{16}$$

where $A1$–$A12$ and $B1$–$B7$ are coefficients given in Appendix B.

3. Solving discrete models

In the following, only the one-degree of freedom model is investigated both theoretically and experimentally. Ordinary differential equations corresponding to discrete models with one or more degrees of freedom are studied using the multiple scales method. In order to maintain the same contribution for the non-linear terms and the damping effect, a small dimensionless parameter ε is used for book-keeping. Hence, the method is used to the first order with the following assumptions:

For one degree of freedom:

$$e = \varepsilon e_0 \quad \text{and} \quad b_i = \varepsilon b_{i0} \quad \text{for } i = 1, \ldots, 7 \tag{17}$$

For two degrees of freedom:

$$A_{20} = A_2, \quad B_{20} = B_2, \tag{18}$$

$$A_i = \varepsilon A_{i0} \quad \text{for } i = 1, 3, \ldots, 12 \tag{19}$$

and

$$B_i = \varepsilon B_{i0} \quad \text{for } i = 1, 3, \ldots, 7. \tag{20}$$

3.1. Primary resonance for 1 d.o.f. model

Assuming, in the usual manner, the frequency expansion as

$$\Omega = \omega_0 + \varepsilon\sigma \tag{21}$$

the approximate solution is obtained via the multiple scales approach

$$\varphi(t) = \rho\cos(\Omega t + v) + o(\varepsilon) \tag{22}$$

with the steady state equations for phase and amplitude verifying:

$$\omega_0(\Omega - \omega_0)\rho - 3\frac{b_2\rho^3}{8} - \frac{b_4}{8}\rho\cos(2v) - \frac{b_4}{4}\rho + \frac{b_5}{2}\cos(v) - \frac{b_7}{2}\sin(v) = 0, \tag{23}$$

$$-\omega_0^2 e\rho + \frac{b_4}{8}\rho\sin(2v) - \frac{b_5}{2}\sin(v) - \frac{b_7}{2}\cos(v) = 0. \tag{24}$$

3.2. Sub-harmonic resonance for the 1 d.o.f. system

Assuming the frequency expansion of the form $\Omega = 2\omega_0 + \varepsilon\sigma$, the multiple scales approach leads to:

$$\varphi(t) = \rho\cos\left(\frac{\Omega}{2}t + v\right) + o(\varepsilon). \tag{25}$$

The steady state equations for phase and amplitude are

$$\frac{(\Omega - 2\omega_0)\omega_0\rho}{2} - 3\frac{b_2\rho^3}{8} - \frac{b_4}{4}\rho - \frac{b_3}{4}\cos(2v)\rho = 0, \tag{26}$$

$$-\omega_0^2 e\rho + \frac{b_3}{4}\rho\sin(2v) = 0. \tag{27}$$

It is important to note that a trivial solution for the equilibrium position is given by $\rho = 0$. Non-trivial solutions are obtained from:

$$\frac{\rho^2}{2} = \frac{2(\Omega - 2\omega_0)\omega_0 - b_4 - \sqrt{b_3^2 - 16(\omega_0^2 e)^2}}{3b_2}, \tag{28}$$

$$\frac{\rho^2}{2} = \frac{2(\Omega - 2\omega_0)\omega_0 - b_4 + \sqrt{b_3^2 - 16(\omega_0^2 e)^2}}{3b_2} \tag{29}$$

with the condition:

$$\frac{b_3^2}{16} - (\omega_0^2 e)^2 \geqslant 0, \tag{30}$$

where b_3 is the parametric term in Eq. (9).

Therefore, for given values of the system parameters, the system may have one or two real solutions for amplitude ρ.

The same kind of analysis could also be carried out for the model with 2 degrees of freedom (see Appendix C).

3.3. Stability analysis of the sub-harmonic solution for the 1 d.o.f. system

For a sub-harmonic resonance and a one degree of freedom model, the following is used (with the constant pair ρ, v for amplitude and phase respectively):

$$\varphi(t) = \rho \cos\left(\frac{\Omega}{2}t + v\right), \tag{31}$$

where ρ and v are solutions of Eqs. (26) and (27) that includes trivial and non-trivial solutions. Then stability analysis is studied via linearization in the neighbourhood of the equilibrium position by replacing (ρ, v) with $(\rho + \delta\rho, v + \delta v)$ for small $\delta\rho(T_1, \ldots)$ and $\delta v(T_1, \ldots)$. Using the modulation equations expressed with physical parameters (all the quantities have been multiplied by ε) the following system of equations is obtained:

$$\varepsilon \frac{\partial}{\partial T_1}\begin{pmatrix}\delta\rho \\ \delta v\end{pmatrix} = \begin{bmatrix}J_{11} & J_{12} \\ J_{21} & J_{22}\end{bmatrix}\begin{pmatrix}\delta\rho \\ \delta v\end{pmatrix}, \tag{32}$$

where

$$\begin{aligned} J_{11} &= -\omega_0 e + \frac{b_3}{4\omega_0}\sin(2v), \\ J_{12} &= \frac{\rho b_3}{2\omega_0}\cos(2v), \\ J_{21} &= \frac{3b_2}{4\omega_0}\rho, \\ J_{22} &= -\frac{b_3}{2\omega_0}\sin(2v). \end{aligned} \tag{33}$$

Noting that $J_{11} = 0$, gives

$$\mathrm{Tr} = -2\omega_0 e \quad \text{and} \quad \mathrm{Det} = -J_{21}J_{12}, \tag{34}$$

where Tr, Det are the trace and the determinant of the matrix $\mathbf{J}$, respectively. Thus the stability analysis may be studied easily via the determinant:

$$\Delta = (\mathrm{Tr})^2 - 4\,\mathrm{Det}. \tag{35}$$

It should be noted that according to the values of the parameters a trivial branch plus two parabolic branches (one stable and one unstable) could be obtained.

4. Description of the experimental system

The experimental set-up for validating the model and showing the main phenomena is described in this section. A diagram of the set-up for a base excitation along the vertical direction is shown in Fig. 1. The cable tested was 1.905 m long (see Table 1 for the main characteristics of the set-up).

After several tests, a steel wire surrounded by copper wire was chosen instead of a cylindrical rod (see Fig. 2). The main advantage of this kind of test specimen is its relatively heavy weight per unit length in comparison to the metallic rod for a similar flexural rigidity.

Table 1
Main characteristics of the set-up

Length of the cable	$L = 1.905\,\mathrm{m}$
Weight per unit length	$m_c = 0.177\,\mathrm{kg/m}$
Inclination of the cable	$\theta = 27.5^\circ$
Initial stress	$80\,\mathrm{N} < T_0 < 200\,\mathrm{N}$
Powered amplitude	$0.025\,\mathrm{mm} < Z_0 < 0.150\,\mathrm{mm}$
Initial tension	60–180 N
Frequency	$5\,\mathrm{Hz} < \Omega\ < 25\,\mathrm{Hz}$

Fig. 2. Test specimen: steel wire surrounded by copper wire.

At the upper end, a load cell composed of a strain-gauge sensor was inserted between the end of the cable and the fixed anchorage (pillar). The cell was connected to a signal-conditioning amplifier (Vishay 2210) and a digital voltmeter was used to measure the static component of the axial force. During testing, the signal was also plotted on a digital oscilloscope and the static and dynamic components of the axial tension were recorded.

The stress was applied at the lower end. A moving part, including a stressing anchorage for the axial force control system, was linked to the head of a 4700 N Gearing & Watson electro-dynamic shaker via a connecting push-rod. The shaker, with a custom table and air suspension, was used to apply the base excitation matching the imposed displacement of the roadway of the bridge (deck). The moving part was guided vertically by two slide bearings. The shaker was powered by a power control unit (G&W DS4) and a function generator (HP33120A). The displacement of the head of the shaker was monitored and held constant by an accelerometer, as the excitation frequency was varied around the frequency studied.

A specific sub-system (stressing anchorage) composed of a thread, a nut and a compression spring was used for the adjustment of the static axial force in the cable (see Fig. 3). In the working

Fig. 3. Sub-system assembly with the stressing anchorage.

configuration, the sub-system was mechanically locked on the moving part. Due to gravity, the cable was slightly bent in the static configuration and the initial axial force was 4 N.

Measurement of the vertical displacement of the cable was measured with an opto-lineic camera (Sysmat OM5) located at the middle of the cable. The linear-array camera, which detects the presence of the cable without contact (see Fig. 1), is equipped with a hardware-implemented peak detector to locate the position of the cable with respect to a reference point. Measurements were acquired, displayed on a scope and stored in real time at a sampling time of 1/500 s. A low-pass filter (9002 Frequency Devices) was used for filtering and magnifying the signal from a 4096 pixel-cell camera. The accuracy of the signal measured depends to a large extent on the quality of the lenses, the distance between the camera and cable, the cable/board contrast and the amplification of the low-pass filter. In testing mode, a spotlight was used to light the cable while a dark board was placed behind it.

In case of out-of-plane motion, another camera, oriented in the second plane, was used to measure horizontal displacement.

The first linear natural frequencies of the cable were obtained with a classical impulse (low amplitude) response by measuring the frequency spectra. A similar test was used to measure the damping ratio for several initial tensions.

5. Experimental results

Cable parameters such as stiffness, length, angle, etc, are chosen while the influence of other parameters is examined. These other parameters are tension T_0 (so that $H = T_0 \cos\theta$) and the amplitude of excitation Z_0. The changes in the excitation frequency were made very gradually and

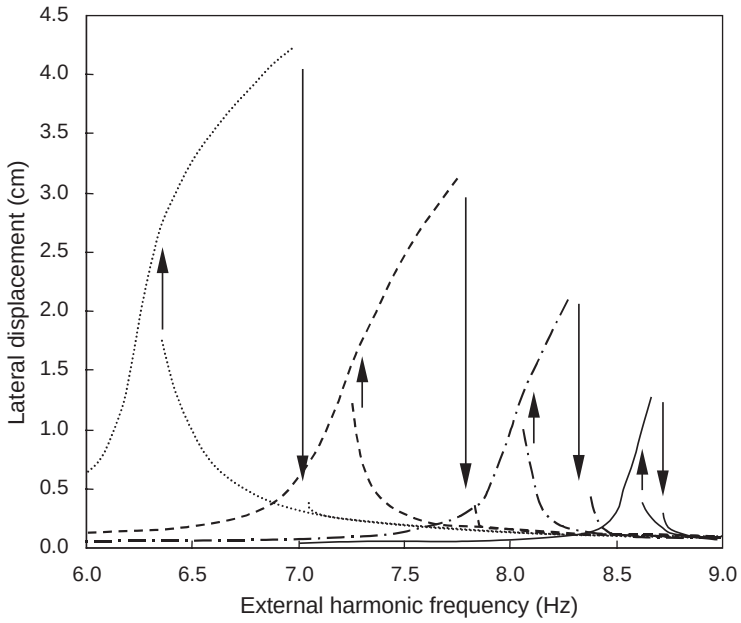

Fig. 4. The influence of varying Z_0 on the primary resonance. Experimental displacements at the middle of the cable for $Z_0 = 0.0125$ mm. (a) $T_0 = 80$ N (⋯⋯), (b) $T_0 = 125$ N (- - - -), (c) $T_0 = 160$ N (– · –) and (d) $T_0 = 185$ N (——).

transients were allowed to die out before the amplitude of the response was recorded. An automatic procedure with a step frequency of 0.01 Hz was used to both increase and decrease the excitation frequency.

5.1. Primary resonance for 1 d.o.f.

5.1.1. Influence of parameters

The experimental results for the primary resonance are given in Fig. 4. In this case, amplitude $Z_0 = 0.075$ mm is weak and tension T_0 has different values from 80 to 180 N. The amplitude of the in-plane vibrations, measured in the middle of the cable with the camera, is plotted versus the excitation frequency. As foreseen, increasing the tension shifted the resonance phenomenon and the jump due to hysteresis, from a weaker frequency (6 Hz) to a higher frequency (9 Hz).

When the tension was fixed at $T_0 = 80$ N, and Z_0 was changed from $Z_0 = 0.025$ to 0.075 mm, two critical effects could be seen (see Fig. 5):

- the amplitude of vibration increased with Z_0, and
- the frequency, where high vibration amplitudes jumped to low vibration amplitudes (hysteresis phenomenon), increased with Z_0.

5.1.2. Comparison theory/experiment

The behaviour is strongly non-linear and from an experimental point of view, the first in-plane or out-of-plane mode vibration of the cable could be observed to alternate for low frequencies

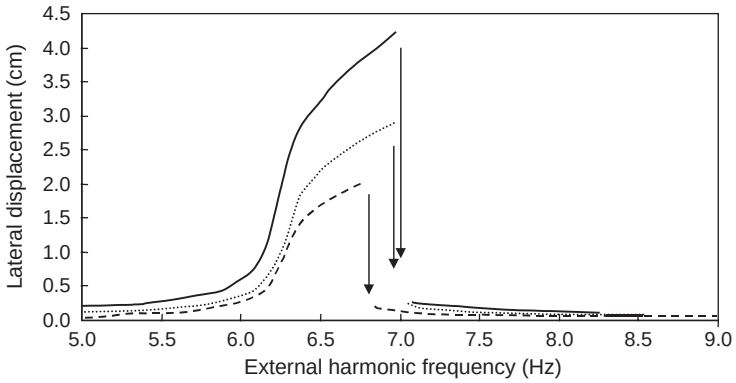

Fig. 5. The influence of varying T_0 on the primary resonance. Experimental displacements at the middle of the cable for $T_0 = 80$ N. (a) $Z_0 = 0.075$ mm (——), (b) $Z_0 = 0,050$ mm (⋯⋯) and (c) $Z_0 = 0.025$ mm (- - -).

(from 5 to 10 Hz) under certain conditions. Since this study is focused on the in-plane mode only, some specific initial conditions may be applied at the beginning of the procedure before obtaining a non-linear stabilized in plane vibration motion, before slowly increasing (or decreasing) the control parameter (the excitation frequency).

The classical hysteresis phenomenon is clearly observed with $H = 80\cos\theta$ N, $\theta = 27.5°$, $Z_0 = 0.05$ mm (see Fig. 6a). For the same parameter values, good qualitative agreement is observed between the experimental results and the approximate theoretical results given by the multiple scale investigation (see Fig. 6b). The quantitative agreement can be obtained if careful consideration is given to the influence of damping and the non-dimensional parameter ξ_0. In fact ξ_0 is not clearly calculated from the theoretical expressions occurring in the model and the measurements from the experimental device. Thus in order to compare the experimental and theoretical results, a procedure is introduced to set the correct parameter ξ_0 and damping in the theoretical model. Therefore ξ_0 is calibrated for the theoretical curve from the experimental results.

The theoretical eigenfrequency ω_0^2 is estimated from the experimental curve with ξ_0, which is computed with Eq. (10), so that the maximal amplitudes are in good agreement. The damping is then also estimated in the theoretical model to calibrate the maximal amplitude of the vibrations. Damping was also measured using a logarithmic decrement from the measured data. The measured and identified parameters are presented in Table 2.

Good quantitative agreement is then obtained between the experiments and the results of the model using identified parameters (see Fig. 7), where the measured and computed amplitudes are plotted versus the frequency of external periodic stresses.

5.2. Results for subharmonic resonance

In this section, the results are presented according to the same procedure as in the previous section. In addition, stability analysis is presented before comparing theoretical and experimental results.

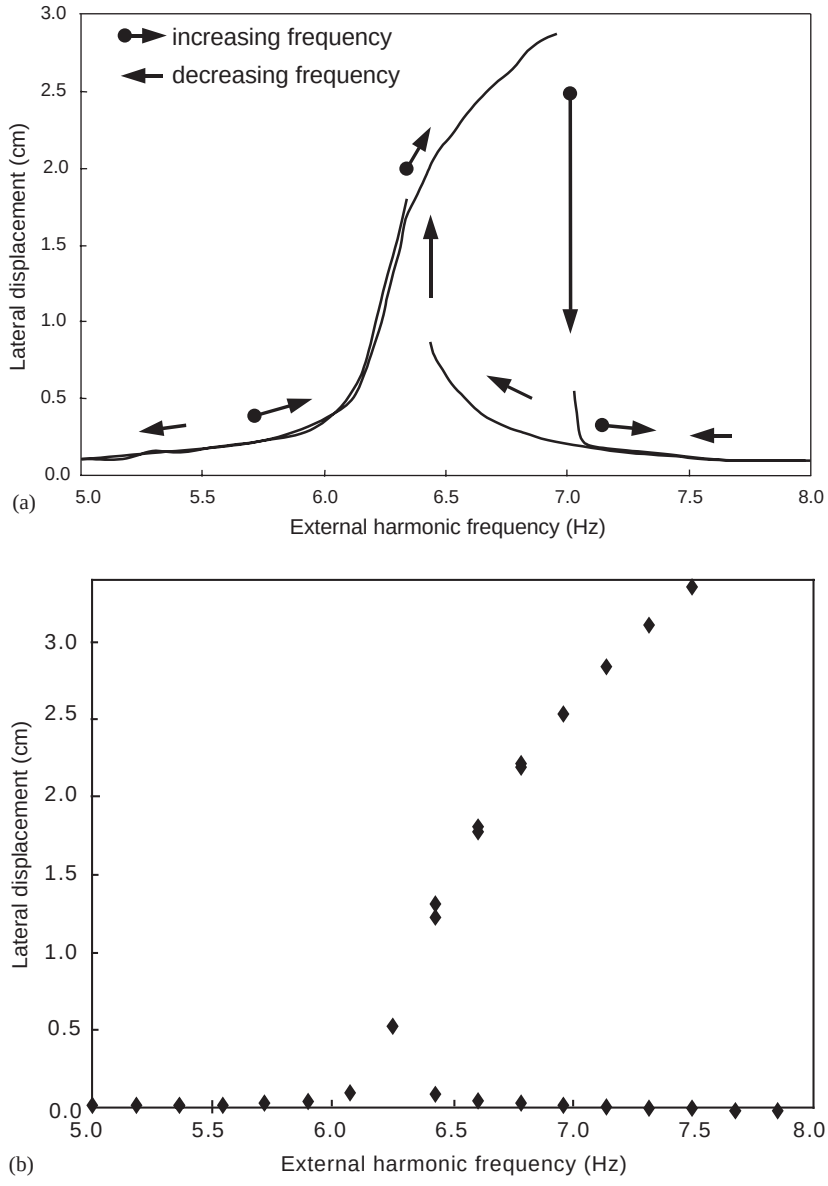

Fig. 6. Primary resonance at the middle of the cable for $T_0 = 80\,\mathrm{N}$; $Z_0 = 0.05\,\mathrm{mm}$: (a) experimental results and (b) fitted (◆).

5.2.1. Influence of parameters

The same parameters (stiffness, length, angle, etc.) as in the previous section are considered. The influence of tension T_0 (with given amplitude Z_0) and the influence of the amplitude of external stress Z_0 (with given tension T_0) on the experimental results are examined.

In Fig. 8, the results are presented for the in-plane vibrations. The amplitude of the displacement (at the middle of the cable) is plotted versus frequency ω close to the subharmonic

Table 2
Comparison between measured and fitted results

	Fitted	Measured
T_0	80 N	80 N
Z_0	0.05 mm	0.05 mm
Frequency	6.3 Hz	6.1 Hz
e	0.6%	0.3–0.5%
ξ_0	From (10)	NA

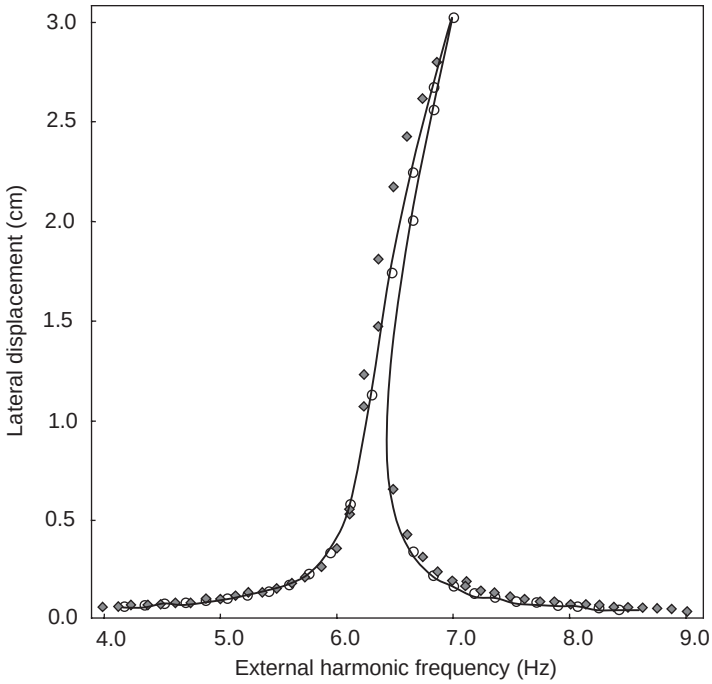

Fig. 7. Primary resonance, amplitude versus excitation frequency: fitted (◦) and experimental (◆).

resonance of order 2, for three different amplitudes of excitation. Supercritical bifurcation curves appear. As can be predicted, the higher Z_0 is, the higher the amplitude is at given frequency ω. This is in agreement with the qualitative behaviour given by the simplified analytical model.

In Fig. 9, the amplitude of the vibrations (at the same location) is presented versus ω, for several values of tension in the cable. The influence of T_0 on the response is that predicted qualitatively by the simplified analytical model: the supercritical parabolic branches start from the trivial branch at a frequency value that increases with T_0. Non-trivial and some parts of trivial branches are obtained by slowly varying the value of the external frequency ω.

The values of the parameters have been chosen so that the sub-harmonic response is 'far from' the frequency value of the second in-plane mode.

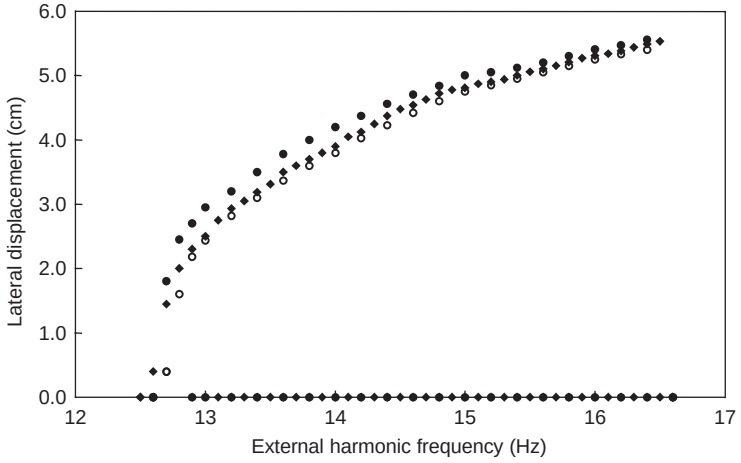

Fig. 8. Sub-harmonic resonance, amplitude versus excitation frequency: $Z_0 = 0.06\,\text{mm}$ (◦), $Z_0 = 0.09\,\text{mm}$ (◆) and $Z_0 = 0.16\,\text{mm}$, (●).

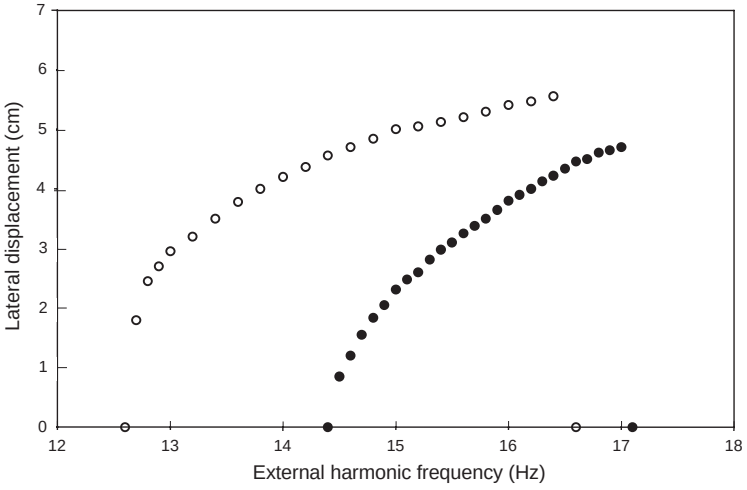

Fig. 9. Sub-harmonic resonance, amplitude versus excitation frequency: $T_0 = 80\,\text{N}$ (◦), $T_0 = 130\,\text{N}$ (●).

5.2.2. *Comparison theory/experiment*

Several experiments were carried out and good qualitative agreement was observed each time. Good quantitative agreement can be obtained if the tension, the damping and Z_0 are prevented from varying during the experiment. In practice, this constancy is difficult to ensure. For instance, when $T_0 = 130\,\text{N}$, $Z_0 = 0.15\,\text{mm}$, $e = 3\%$ and ξ_0 (calculated during experiments), some small fluctuations occur so that Z_0 is in the range [0.15:0.155 mm] and T_0 in the range [130 N:135 N]. Thus, the eigenfrequency measured is 7.4 Hz (theoretical value: 7.2 Hz).

The results for such an experiment are given in Fig. 10, where the amplitude (at $L/2$) is plotted versus ω and good quantitative agreement is obtained. It should be noted that in some

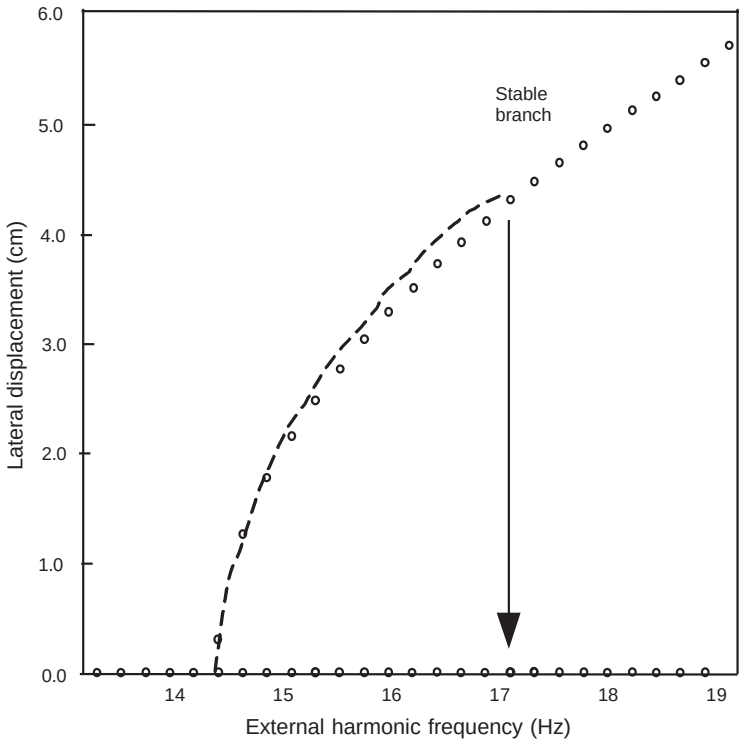

Fig. 10. Sub-harmonic resonance, amplitude versus excitation frequency, experiment (—) and theoretical stable branch (○).

experimental results (not presented here) the stable branch does not persist because of the occurrence of higher (in-plane or out-of-plane) modes.

6. Conclusions

This paper presented a modified model for the dynamic behaviour of an inclined cable. Both primary and sub-harmonic resonances have been studied from a theoretical point of view by using the multiple scales method. The one degree of freedom model is devoted to in-plane motion and is easily extended to 2 degrees of freedom for in-plane and out-of-plane motions. The model has been validated from the experimental point-of-view on a specific set-up using a shaker and contactless sensors. Due to potential applications in the field of civil engineering, the influence of parameters such as tension and amplitude of external excitation (corresponding to the motion of a bridge deck) has been presented. The results presented show good agreement between prediction and experimentation and validate the model. Sophisticated dynamical behaviours have been observed in the setup for coupled and uncoupled motions. Further investigations of the two degrees of freedom model and analytical developments have to be carried out in order to study the

contribution of coefficients of non-linear terms and parametric terms in the mathematical model. In addition, it may be interesting to discuss and study the effect of external stochastic excitation.

Acknowledgements

The authors would like to thank Franck Bourrier and Christophe Quesne who provided part of the experiment and the numerical computation.

Appendix A. Coefficient for the simplified model with one degree of freedom

The first eigenfrequency ω_0 of the cable is obtained from [7]:

$$\mathrm{tg}\left(\frac{\omega_0}{2}\right) = \frac{\omega_0}{2} - \frac{4}{\lambda^2}\left(\frac{\omega_0}{2}\right)^3 \tag{A.1}$$

with

$$\lambda^2 = \frac{\xi_0 \eta_0^2}{1 + (\eta_0^2/8)} \tag{A.2}$$

and

$$\eta_0 = \frac{8\zeta}{\cos^2\theta} \quad \text{and} \quad \gamma = \frac{\zeta}{L}, \tag{A.3}$$

where ζ corresponds to the deflection at middle of the cable.

Coefficients $b_1, \ldots, b_7$ and $C_0, \ldots, C_3$ are given by

$$\begin{aligned} b_1 &= \frac{3C_1C_2}{2C_0}\gamma\xi, \quad b_2 = \frac{C_1^2}{2C_0}\gamma^2\xi, \quad b_3 = \frac{C_1}{C_0}\xi\gamma Z_0 \sin\theta, \\ b_4 &= \frac{C_1}{2C_0}\xi\gamma^2 Z_0^2 \cos^2\theta, \quad b_5 = \frac{Z_0}{C_0}(C_3\Omega^2\cos\theta - C_2\xi\sin\theta), \\ b_6 &= -\frac{C_2}{2C_0}\xi\gamma Z_0^2\cos^2\theta, \quad b_7 = \frac{C_3}{C_0}2\mathrm{e}\omega_0\Omega Z_0\cos\theta, \end{aligned} \tag{A.4}$$

$$\begin{aligned} C_0 &= \int_0^1 f^2(X)\,\mathrm{d}X \quad C_1 = \int_0^1 f'^2(X)\,\mathrm{d}X, \\ C_2 &= \int_0^1 f'(X)Y'\,\mathrm{d}X \quad C_3 = \int_0^1 Xf(X)\,\mathrm{d}X. \end{aligned} \tag{A.5}$$

Appendix B. Coefficient for the simplified model with two degree of freedom

$$A1 = c_1\gamma\sqrt{\frac{T_0}{m_c}},\ \ A2 = \frac{C_1}{C_0} + \xi\frac{C_2^2}{C_0},\ \ A3 = \frac{C_1}{C_0}\xi\gamma Z_0\sin\theta,$$
$$A4 = \frac{C_1}{2C_0}\xi\gamma^2 Z_0^2\cos^2\theta,\ \ A5 = \frac{C_1^2}{2C_0}\gamma^2\xi,\ \ A6 = \frac{3C_1C_2}{2C_0}\gamma\xi,$$
$$A7 = \frac{C_2C_4}{2C_0}\gamma\xi.\ \ A8 = \frac{C_1C_4}{2C_0}\gamma^2\xi.\ \ A9 = \frac{Z_0}{C_0}C_2\xi\sin\theta,$$
$$A10 = \frac{C_2}{2C_0}\xi\gamma Z_0^2\cos^2\theta,\ \ A11 = -\frac{C_3}{C_0}e_1 Z_0\cos\theta,\ \ A12 = -\frac{C_3}{C_0}Z_0\cos\theta, \tag{B.1}$$

$$B1 = c_2\gamma\sqrt{\frac{T_0}{m_c}},\ \ B2 = \frac{C_4}{C_5},\ \ B3 = \frac{C_4}{C_5}\xi\gamma Z_0\sin\theta,$$
$$B4 = \frac{C_4}{2C_5}\xi\gamma^2 Z_0^2\cos^2\theta,\ \ B5 = \frac{C_4^2}{2C_5}\gamma^2\xi,\ \ B6 = \frac{C_2C_4}{C_5}\gamma\xi,$$
$$B7 = \frac{C_1C_4}{2C_5}\gamma^2\xi, \tag{B.2}$$

where local coefficients C_0 and C_5 are as follow:

$$C_0 = \int_0^1 f_y^2(X)\,\mathrm{d}X,\ \ C_1 = \int_0^1 f_y'^2(X)\,\mathrm{d}X,\ \ C_2 = \int_0^1 f_y'(X)\,Y'\,\mathrm{d}X,$$
$$C_3 = \int_0^1 Xf_y(X)\,\mathrm{d}X,\ \ C_4 = \int_0^1 f_z'^2(X)\,\mathrm{d}X,\ \ C_5 = \int_0^1 f_z^2(X)\,\mathrm{d}X. \tag{B.3}$$

Appendix C. Model with two degrees of freedom

C.1. Primary resonance for a 2 d.o.f. system

Assuming that frequencies ω_p and ω_{op} of the in-plane and out-of-plane respectively are close to each other

$$\omega_p = \sqrt{A20}, \tag{C.1}$$

$$\omega_{op} = \sqrt{B20} = \sqrt{A20} + \varepsilon v. \tag{C.2}$$

The primary resonance corresponds to

$$\Omega = \omega_p + \varepsilon\sigma \tag{C.3}$$

and the multiple scales in time method provides solutions in the form:

$$\varphi_y = a\cos(\Omega t + \alpha), \tag{C.4}$$

$$\varphi_z = b\cos(\Omega t + \beta), \tag{C.5}$$

where a, b, α and β verify

$$\begin{aligned}
&a\omega_p(\Omega - \omega_p) - \tfrac{3}{8}A5a^3 - \tfrac{1}{8}A4a\cos(2\alpha) - \tfrac{1}{4}A4a - \tfrac{1}{2}\cos(\alpha)(A9 + \Omega^2 A12)\\
&\quad + \tfrac{1}{2}A11\sin(\alpha)\Omega - \tfrac{1}{4}A8ab^2 - \tfrac{1}{8}A8ab^2\cos(2\alpha - 2\beta) = 0,\\
&-\tfrac{1}{2}A1a\omega_p + \tfrac{1}{8}A4a\sin(2\alpha) + \tfrac{1}{2}\sin(\alpha)(A9 + \Omega^2 A12) + \tfrac{1}{2}A11\cos(\alpha)\Omega\\
&\quad + \tfrac{1}{8}A8ab^2\sin(2\alpha - 2\beta) = 0,\\
&b[\omega_p(\Omega - \omega_{op}) - \tfrac{3}{8}B5b^2 - \tfrac{1}{8}B4\cos(2\beta) - \tfrac{1}{4}B4 - \tfrac{1}{4}B7a^2 - \tfrac{1}{8}B7a^2\cos(2\alpha - 2\beta)] = 0,\\
&b[-\tfrac{1}{2}B1\omega_p + \tfrac{1}{8}B4\sin(2\beta) - \tfrac{1}{8}B7a^2\sin(2\alpha - 2\beta)] = 0.
\end{aligned} \tag{C.6}$$

C.2. Sub-harmonic motions for a 2 d.o.f. system

Again assuming ω_p and ω_{op} are close together and

$$\Omega = 2\omega_p + \varepsilon\sigma \tag{C.7}$$

solutions in the form:

$$\varphi_y = a\cos\left(\frac{\Omega}{2}t + \alpha\right), \tag{C.8}$$

$$\varphi_z = b\cos\left(\frac{\Omega}{2}t + \beta\right) \tag{C.9}$$

are obtained, with

$$\begin{aligned}
&a\left[\omega_p\left(\frac{\Omega}{2} - \omega_p\right) - \tfrac{3}{8}A5a^2 - \tfrac{1}{4}A4 - \tfrac{1}{4}A3\cos(2\alpha) - \tfrac{1}{4}A8b^2 - \tfrac{1}{8}A8b^2\cos(2\alpha - 2\beta)\right] = 0,\\
&a\left[-\tfrac{1}{2}A1\omega_p + \tfrac{1}{4}A3\sin(2\alpha) + \tfrac{1}{8}A8b^2\sin(2\alpha - 2\beta)\right] = 0,\\
&b\left[\omega_p\left(\frac{\Omega}{2} - \omega_{op}\right) - \tfrac{3}{8}B5b^2 - \tfrac{1}{4}B4 - \tfrac{1}{4}B3\cos(2\beta) - \tfrac{1}{4}B7a^2 - \tfrac{1}{8}B7a^2\cos(2\alpha - 2\beta)\right] = 0,\\
&b\left[-\tfrac{1}{2}B1\omega_p + \tfrac{1}{4}B3\sin(2\beta) - \tfrac{1}{8}B7a^2\sin(2\alpha - 2\beta)\right] = 0.
\end{aligned} \tag{C.10}$$

References

[1] C. Carasso, M. Rascle, D. Serre, Etude d'un modèle hyperbolique en dynamique des câbles, *Mathematical Modelling and Numerical Analysis* 19 (4) (1985) 573–599.

[2] B. Portier, Dynamic phenomena in ropeways after a haul rope rupture, *Earthquake Engineering and Structural Dynamics* 12 (1984) 433–449.

[3] J. Coomer, M. Lazarus, R.W. Tucker, D. Kershaw, A. Tegman, A non-linear eigenvalue problem associated with inextensible whirling strings, *Journal of Sound and Vibration* 239 (5) (2001) 968–982.

[4] Y.L. Xu, Z. Yu, Non-linear vibration of cable-damper systems Part I: formulation, *Journal of Sound and Vibration* 225 (3) (1999) 447–463.

[5] Y.L. Xu, Z. Yu, Non-linear vibration of cable-damper systems Part II: application and verification, *Journal of Sound and Vibration* 225 (3) (1999) 465–481.
[6] Y. Achkire, Active Tendon Control of Cable-stayed Bridges, Ph.D., Université libre de Bruxelles, Faculty of Sciences, 1997, 121p.
[7] H.M. Irvine, T.K. Caughey, The linear theory of free vibrations of a suspended cable, *Proceedings of the Royal Society of London A* 341 (1974) 299–315.
[8] H.M. Irvine, *Cable Structures*, The M.I.T. Press, Cambridge, MA, 1981.
[9] G.F. Carrier, On the non-linear vibration problem of the elastic string, *Quarterly Applied Mathematics* 3 (1945) 157–165.
[10] G.F. Carrier, A note on the vibration string, *Quarterly Applied Mathematics* 7 (1949) 97–101.
[11] L. Meirovitch, *Elements of Vibration Analysis*, McGraw-Hill, New York, 1975.
[12] H.H. West, L.F. Geschwindner, J.E. Suhoski, Natural vibrations of suspension cables, *Journal of the Structural Division* ST11 (1975) 2277–2291.
[13] W.M. Henghold, J.J. Russell, Equilibrium and natural frequencies of cable structures (A nonlinear finite element approach), *Computers & Structures* 6 (1976) 267–271.
[14] A.H. Nayfeh, D.T. Mook, *Nonlinear Oscillations*, Wiley, New York, 1979.
[15] K. Takahashi, Y. Konishi, Non-linear vibrations of cables in three dimensions, Part I: non-linear free vibrations, *Journal of Sound and Vibration* 118 (1) (1987) 69–84.
[16] K. Takahashi, Y. Konishi, Non-linear vibrations of cables in three dimensions, Part II: out of plane vibrations under in-plane sinusoidally time-varying load, *Journal of Sound and Vibration* 118 (1) (1987) 85–97.
[17] F. Benedettini, G. Rega, Planar non-linear oscillations of elastic cables under superharmonic resonance conditions, *Journal of Sound and Vibration* 132 (3) (1989) 353–366.
[18] G. Rega, F. Benedettini, Planar non-linear oscillations of elastic cables under subharmonic resonance conditions, *Journal of Sound and Vibration* 132 (3) (1989) 367–381.
[19] F. Benedettini, G. Rega, Non-linear dynamics of an elastic cable under planar excitation, *International Journal of Nonlinear Mechanics* 22 (1987) 497–509.
[20] F. Benedettini, F. Vestroni, G. Rega, Parametric analysis of large amplitude free vibrations of a suspended cable, *International Journal of Solids and Structures* 20 (2) (1984) 95–105.
[21] F. Benedettini, G. Rega, R. Alaggio, Non-linear oscillations of a four-degree-of-freedom model of a suspended cable under multiple internal resonance conditions, *Journal of Sound and Vibration* 182 (5) (1995) 775–798.
[22] G. Rega, W. Lacarbonara, A.H. Nayfeh, Char-Ming Chin, Multimodal resonances in suspended cables via a direct perturbation approach, *Proceedings of ASME DETC97*, Vol. DETC97/VIB-4101, Sacramento, CA, September 14–17, 1997.
[23] V.N. Pilipchuk, R.A. Ibrahim, Non-linear modal interactions in shallow suspended cables, *Journal of Sound and Vibration* 227 (1) (1999) 1–28.
[24] G. Zheng, J.M. Ko, Y.Q. Ni, Super-harmonic and internal resonances of a suspended cable with nearly commensurable natural frequencies, *Nonlinear Dynamics* 30 (2002) 55–70.
[25] O.M. Reilly, Global bifurcations in the forced vibration of a damped string, *International Journal of Non-Linear Mechanics* 28 (3) (1993) 337–351.
[26] J.L. Lilien, A. Pinto da Costa, Vibration amplitudes caused by parametric excitation of cable stayed structure, *Journal of Sound and Vibration* 174 (1) (1994) 69–90.
[27] Y. Fujino, P. Warnitchai, B.M. Pacheco, An experimental and analytical study of autoparametric resonance in a 3 DOF model of cable-stayed-beam, *Nonlinear Dynamics* 4 (1992) 111–138.
[28] I. Khadraoui, Contribution à la Modélisation et à l'Analyse Dynamique des Structures à Câbles, Thèse de Doctorat, Université d'Evry, 1999 (in French).
[29] Y.Y. Zhao, L.H. Wang, D.L. Chen, L.Z. Jiang, Non-linear dynamics analysis of the two-dimensional simplified model of an elastic cable, *Journal of Sound and Vibration* 255 (1) (2002) 43–59.
[30] S.R.K. Nielsen, P.H. Kirkegaard, Super and combinatorial harmonic response of flexible elastic cables with small sag, *Journal of Sound and Vibration* 251 (1) (2002) 79–102.

[31] A.I. Raouf, Stochastic dynamics of the Duffing oscillator with applications to strings and cables, in: J.M. Balthazar, P.G. Gonçalves, R.M.F.L.R. Brasil, I.L. Caldas, F.B. Rizatto (Eds.), *Nonlinear Dynamics, Chaos, Control, and their Applications to Engineering Sciences*, Vol. 4, Associação Brasileira Mecânicas, Rio de Janeiro, 2002, pp. 1–39.

[32] A. Berlioz, C.H. Lamarque, J.M. Malasoma, Non linear behavior of an inclined cable: experimental and analytical investigations, *Proceedings of ASME DETC2001*, Vol. DETC2001/VIB-21557, Pittsburgh, PA, September 9–12, 2001.